Piece by Piece - Electrochemical Synthesis of Individual Nanoparticles and their Performance in ORR Electrocatalysis

*Mathies V. Evers, Miguel Bernal, Beatriz Roldan Cuenya, and Kristina Tschulik**

[*] M. V. Evers, Dr. M. Bernal, Prof. Dr. K. Tschulik
Ruhr University Bochum, Faculty of Chemistry and Biochemistry Chair of Analytical Chemistry II
44801 Bochum (Germany), E-mail: Kristina.Tschulik@rub.de
Prof. Dr. B. Roldan Cuenya Department of Interface Science
Fritz Haber Institute of the Max Planck Society 14195 Berlin (Germany)

Abstract:
The impact of individual HAuCl4 nanoreactors is measured electrochemically, which provides operando insights and precise control over the modification of electrodes with functional nanoparticles of well-defined size. Uniformly sized micelles are loaded with a dissolved metal salt. These solution- phase precursor entities are then reduced electrochemically— one by one—to form nanoparticles (NPs). The charge transferred during the reduction of each micelle is measured individually and allows operando sizing of each of the formed nanoparticles. Thus, particles of known number and sizes can be deposited homogenously even on nonplanar electrodes. This is demonstrated for the decoration of cylindrical carbon fibre electrodes with 25 : 7 nm sized Au particles from HAuCl4-filled micelles. These Au NP-decorated electrodes show great catalyst performance for ORR (oxygen reduction reaction) already at low catalyst loadings. Hence, collisions of individual precursor-filled nanocontainers are presented as a new route to nanoparticle-modified electrodes with high catalyst utilization.

Nanoparticles (NPs) are a major interdisciplinary research field as their synthesis and characterisation continue to pose challenges.[1–3] Since the size is crucial to their properties, the production of monomodal NP batches with narrow size distribution is highly desired to maximise catalytic activity and selectivity.[4,5] Simultaneously, costs related to the usage of precious metals are reduced. Micelles as templates enable size-selective syntheses. There, a well-defined amount of precursor is confined in a container of a specific size. Very uniformly sized micelles can be produced, utilizing diblock copolymers,[6,7] and filled with metal salt solutions as pre- cursors. These micellar nanoreactors move about freely in solution and will sporadically collide with an electrode immersed in this solution by virtue of Brownian motion. Here we show that during these individual collisions, the precursor contained inside the micelle[8] can be electrochemi- cally reduced and deposited as a NP at the electrode. The electrochemical charge transferred during each of these impact events allows us to determine the size of the formed NPs one by one. The number of events recorded determines the number of NPs formed. Thanks to the random-walk- driven collisions, a

homogeneous coverage of a substrate is achieved during such nano-impacts, even for complex substrate shapes. This is highly desirable to achieve maximum NP utilization in electrocatalysis and sensing.[9]

In the literature, individual impact electroanalysis[10,11] is divided into non-Faradaic capacitive or blocking experiments, and Faradaic catalytic or destructive experiments. These describe the charging, the decrease in electroactive area, catalysis, and consumption of NPs, respectively.[12–15] In contrast to these categorised procedures, we present the controlled synthesis of NPs that occurs in individual events. This tool enables real-time solution-phase analysis of the deposition event at the solid–liquid interface of the electrode. Conventionally, micelle-confined precursors are reduced chemically using $NaBH_4$, N_2H_4, H_2S, other reductants, or physically by thermal decomposition.[16,17] Major drawbacks of chemical reduction are the contamination of the resulting NP batch and the difficulty of monitoring the reduction process.[18] Moreover, it is difficult to control and determine the number and size of individual NPs formed upon chemical reduction of micelles in situ. In nanopatterning, complex substrate morphology and the limits of galvanic exchange pose the limiting factors.[19]

These drawbacks are circumvented in the electrochemical approach used in this work. Precise control of the reduction strength and reaction rate is gained by the applied electrode potential. Instead of a chemical reducing agent, the electrode serves as the electron source with a controlled Fermi level. The reaction is driven for a desired duration, wherein both the number of impacting micelles and transferred charge are monitored. This enables real-time control of NP size and coverage. Also, microemulsion droplets, where a second liquid phase is introduced, may be used for this approach.[20–24] However, micelles may be advantageous, as a lower polydis- persity index and a longer shelf-life can be achieved in comparison to ultrasonication-derived microemulsions.[25] As shown below, the micellar polymer does not measurably influence the catalytic activity in the presented case.

The herein described nanoreactor impact method is more generally applicable than galvanic exchange and does not incorporate additional metals that can influence the envis- aged application. Further, decoration of any electrically conducting substrate is readily achievable, including non-planar electrodes with high aspect ratios that are not suitable for spin coating, for instance.

We employ the new method of impact electrochemistry to monitor the size and number of individually deposited NPs in
real time. Using the oxygen reduction reaction (ORR), it is then shown that the modified carbon fibres prepared this way show excellent catalyst performance already at a low gold coverage of approximately 11 %.

Firstly, micelles of well-defined volume were prepared and filled with a gold precursor, and their successful loading and size distribution was determined ex situ. See Section 1 in the Supporting Information for experimental details.

In brief, reverse micelles of the diblock co-polymer P2VP- PS (poly-2-vinylpyridine polystyrene) with adjustable and narrow monomodal size distribution were prepared in toluene, as described by Behafarid et al.,[7] and loaded with a precursor by addition of chloroauric acid ($HAuCl_4$). Chloroauric acid is insoluble in toluene and accumulates within the micelles, which thus serve as precursor nanoreactor cages. SEM (scanning electron microscopy) and AFM (atomic force microscopy) analysis of $HAuCl_4$@P2VP-PS revealed a nanocage size of 59 +/- 10 nm (see Supporting Information Figure S1), which is an order of magnitude smaller and much more well-defined than microemulsion droplets. In order to measure their gold content, micelles were dip-coated on a silicon wafer and treated in oxygen plasma to remove all polymer and form Au NPs.[26] The size of the NPs was 20 : nm, as shown in the AFM image in Figure 1.

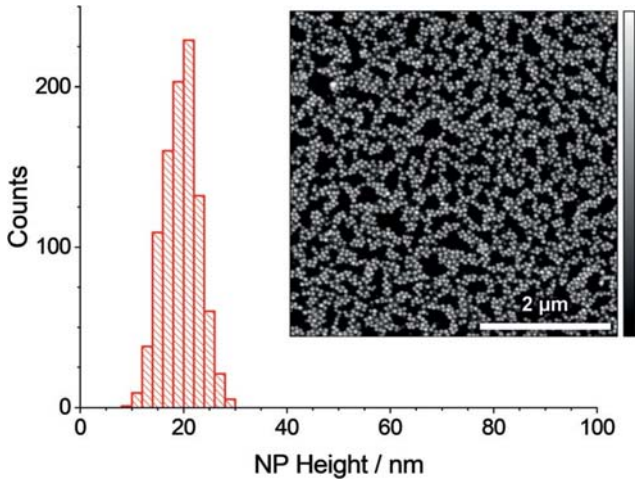

Figure 1. NP height histogram and corresponding AFM image of O_2- plasma-cleaned Au NPs from $HAuCl_4$@P2VP-PS micelles on SiO_2/ Si(111).

Secondly, electrochemical ensemble measurements were used to identify a suitable potential to reduce the precursor ($HAuCl_4$) in the micelles to gold. The inverse micelles were redispersed from toluene into the ionic liquid 1-ethyl-3- methylimidazolium bis(trifluoromethylsulfonyl)imide $[C_2C_1im][NTf_2]$, as described in Section 1.3 in the Supporting Information. After the removal of toluene, a three-electrode system was introduced to record the linear sweep voltammo- grams (LSVs) shown in Figure 2 on Pt and C microelectrodes. The potential was driven from 0 V vs. a Pt quasi-reference electrode (PtQRE) to negative potentials with a scan rate of 0.1 Vs^{-1}. On Pt (Figure 2 A), the micellar $HAuCl_4$@P2VP-PS is reduced to Au^0 (peak I, red) in a single-wave reduction, whereas nonconfined $HAuCl_4$ exhibits a double-wave electro- reduction (I and II, black). The reduction of $HAuCl_4$ in micelles (I, red) occurs at a potential about 300 mV less negative than that without micelles (peak II in black). On a carbon electrode (Figure 2 B) this difference shrinks to ca. 150 mV. The micellar environment leads to full electro- reduction at an earlier potential, which is subsequently used for the individual electrodeposition of nanoparticles (vide infra).

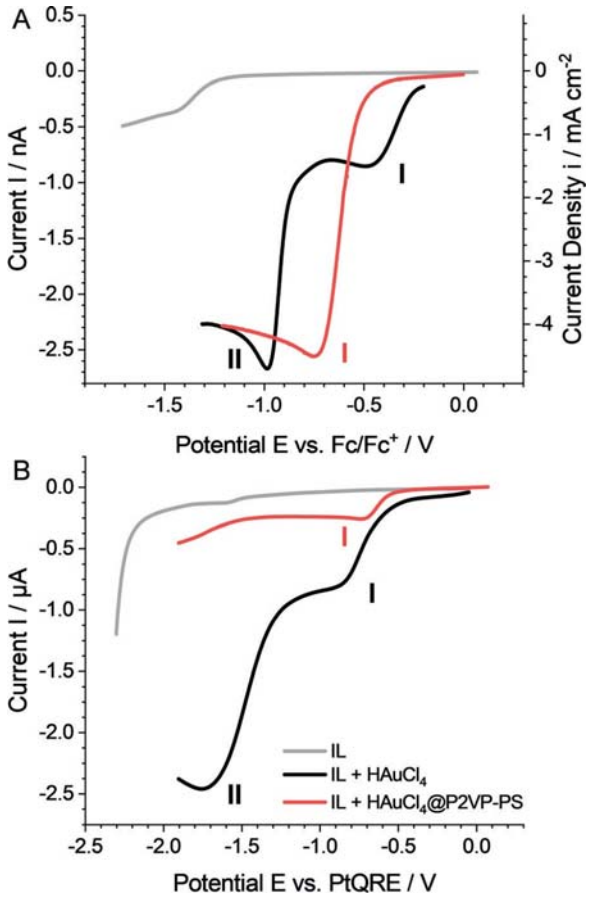

Figure 2. Linear sweep voltammograms (LSV) of HAuCl4@P2VP-PS micelles in [C2C1im][NTf2]; scan rate 0.1 Vs@1. A) LSV at a Pt microdisk (Ø 8 mm), potential referenced against internal redox couple ferrocene/ ferrocenium. B) LSV at cylindrical C microfibre (Ø 7 mm).

Next, we use nano-impact experiments to synthesise Au NPs from $HAuCl_4$@P2VP-PS micelles, while simultaneously measuring their individual size. In this novel synthesis approach, which we call "constructive nano-impact," the micelles are allowed to diffuse to the electrode via Brownian motion. Upon the stochastic impact of each individual micelle at a negatively polarised Pt microdisk electrode (E = -1.09 V vs. Fc/Fc^+, 3-electrode setup), the precursor contained in the micelle is electrochemically reduced. Accordingly, each measured transient current response (spike) marks the electrodeposition of an individual Au NP on the electrode. This reduction spike in the current–time trace is integrated $\int I dt$ to measure the charge Q. In accordance with the chemical reaction [Eq. (1)][27] and Faraday◊s laws of electrol- ysis, the charge Q is directly related to the amount of Au^0 deposited. Since the NPs were mostly spherical in shape (see Figures 1 and 3), the charge directly translates into the diameter d via the sphere volume V [Eq. (2)],[28] where 1 denotes the density of Au, M the molar mass of Au, z the number of transferred electrons, and F the Faraday constant.

$$HAuCl_4 + 3e^- \rightarrow Au_0 + H^+ + 4Cl^- \qquad (1)$$

$$d = 2 \cdot \sqrt[3]{3V/4\pi} = 2 \cdot \sqrt[3]{(3QM)/(4\pi\rho zF)} \qquad (2)$$

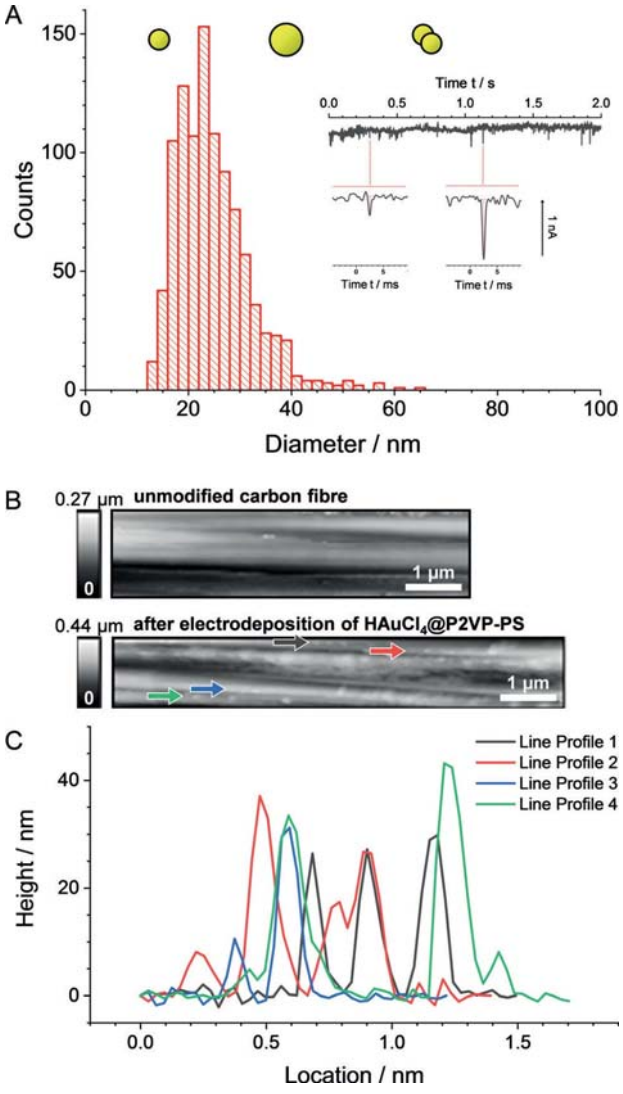

Figure 3. A) Size histogram of NPs electrodeposited by nano-impacts on a cylindrical carbon microfibre; data of 1014 impacts. Inset shows the current transient during an impact measurement and enlarged views of two impact features; additional examples are provided in Figure S4 in the Supporting Information. B) AFM image of a cylindrical C fibre before and after impact decoration. C) Baseline-corrected line profiles of the height channel show the size of NPs deposited on the C fibre.

From a total of 1014 individual micelle impacts, a size histogram of the formed NPs was plotted. It yielded an average diameter of 25 7 nm (Figure 3 A). This is in excellent agreement with the Au NP size obtained ex situ from plasma-treated micelles (20 3 nm, Figure 1), thus confirming the quantitative conversion of the precursor material in each micelle during the nano-impacts. Only few agglomerates were seen at larger diameters. AFM analysis of a cylindrical carbon microfibre decorated by nano-impacts validates the measured size (Figure 3 B), which is further confirmed by deposition on a flat substrate (highly oriented pyrolytic graphite, Figure S3 in the Supporting Information). Constructive impacts were run for a series of deposition times to determine the coverage of a C fibre electrode as a function of the modification time (Figure 4).

We found that the amount of Au homogeneously deposited from $HAuCl_4$@P2VP-PS increased and converged towards satura- tion up to 100 s. At very long durations a greatly increased amount of Au was observed (see Figure S2). Hence, a limiting "monolayer-type" deposition is assumed, followed by multi- layer formation in analogy to classical Brunauer–Emmett– Teller (BET) behaviour. Both SEM and AFM analysis of the modified electrodes revealed deposited Au NPs of spherical shape. Thus, we demonstrated that $HAuCl_4$@P2VP-PS elec- trodeposition leads to reproducibly sized particles, which is in stark contrast to Au NPs from non-confined $HAuCl_4$. Furthermore, the particles adhered strongly to the electrode, allowing us to use the particle-decorated electrodes in catalysis, namely the ORR.

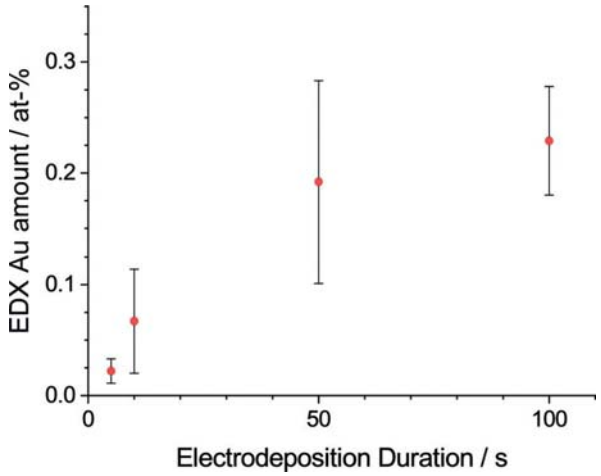

Figure 4. Amount of Au deposition over time after electroreduction of HAuCl4@P2VP-PS micelles on C microfibres; values measured by EDX relative to the detected carbon content (see Section 3.1 in the Supporting Information).

Bulk Au catalyses ORR greatly with respect to blank C fibre electrodes,[29] which is seen from the earlier onset potential at which the reaction starts to show measurable current. Since the kinetics of ORR electrocatalysis on Au NPs were studied in detail previously,[29] we utilised

carbon microfibre electrodes modified with Au NPs in ORR catalysis as a model system herein. First, Au NPs were deposited on a C fibre by micellar nano-impacts and the residual ionic liquid was removed. Next, the decorated fibres were transferred to 0.1m H_2SO_4 for ORR studies. Using linear sweep voltammetry, the ORR onset potential was determined for Au NPs in comparison to a bare C fibre and a polycrystalline Au electrode, respectively. The measured current was normalized by the surface area, corrected for the hydrogen evolution reaction (HER) in deaerated measurements, and plotted in Figure 5. For the decorated C electrodes, the surface area of (Figure 5 B).

The exceptionally high performance of few, homogeneously distributed NPs is thus clearly demonstrated. Note that this does not prove NPs to be more active than bulk Au, but the improvement may (partially) be caused by the efficient hemispherical mass transport of reactants to the individual catalyst NPs. In fact, calculation of the kinetic parameters of our micelle-born Au NPs shows they have identical catalytic activity for ORR as the capping-agent-free Au NPs reported by Wang et al.[29] This confirms that the micellar polymer does not hamper the catalytic activity of the synthesized NPs, as predicted by Behafarid et al.[7]

In the present work, we demonstrate that micelles can be used as precursor nanoreactor cages to electrosynthesise NPs of narrow size distribution. To homogenously coat Au NPs onto substrate electrodes, we developed and employed the concept of "constructive nano-impacts", which describes the electroreduction of individual precursor-filled nanoreactors during their impact at the substrate meant to be decorated. This new electrosynthesis tool allows us to deposit NPs one by one and monitor the size and the number of individual NPs formed in situ based on their individual current response. This approach facilitates the highly efficient utilization of precious metal catalysts, as evidenced for micelle-derived Au NPs in ORR catalysis. At the same time, these modified electrodes are ideal model electrodes for numerical simulations to extract quantitative physicochemical insights on reaction kinetics and mass transport at nonplanar electrodes.

As the micelle can be used to store a variety of different precursor substances and mixtures thereof, this novel concept of constructive nano-impacts also provides a route to produce a variety of NP-modified electrodes. The monomodal size distribution of the micelles and the homogeneous and precisely adjustable NP surface coverage enable the produc- tion of high-performance, low-cost electrodes for electro- catalytic and electrochemical sensing applications. We antici- pate that this will lead to improvements in fuel cells, water purifiers, and toxin detectors amongst other devices.

Acknowledgements

This work was financially supported by the NRW Rückkehrerprogramm and by the Deutsche Forschungsgemeinschaft (DFG) under Germany's Excellence Strategy EXC-2033 Project-#390677874 and the Research Training Group 'Confinement-controlled Chemistry' GRK2376/ 331085229. M. B. acknowledges funding from IMPRS-SURMAT, BMBF under Grant #03F0523C-"CO2EKAT" and the ERC under Grant ERC-OPERANDOCAT (ERC-725915).

Conflict of interest

The authors declare no conflict of interest.

Keywords

gold nanoparticles
ionic liquids
micelles
nanoparticle collision experiments
oxygen reduction reaction

References

1. S. P. Shields, V. N. Richards, W. E. Buhro, *Chem. Mater.* 2010, *22*, 3212 – 3225.
2. E. N. Saw, V. Grasmik, C. Rurainsky, M. Epple, K. Tschulik, *Faraday Discuss.* 2016, *193*, 327 – 338.
3. V. Grasmik, C. Rurainsky, K. Loza, M. V. Evers, O. Prymak, M. Heggen, K. Tschulik, M. Epple, *Chem. Eur. J.* 2018, *24*, 9051 – 9060.
4. R. Reske, H. Mistry, F. Behafarid, B. Roldan Cuenya, P. Strasser, *J. Am. Chem. Soc.* 2014, *136*, 6978 – 6986.
5. H. S. Jeon, I. Sinev, F. Scholten, N. J. Divins, I. Zegkinoglou, L. Pielsticker, B. Roldan Cuenya, *J. Am. Chem. Soc.* 2018, *140*, 9383 –9386.
6. A. H. Gröschel, A. Walther, *Angew. Chem. Int. Ed.* 2017, *56*, 10992 – 10994; *Angew. Chem.* 2017, *129*, 11136 – 11138.
7. F. Behafarid, J. Matos, S. Hong, L. Zhang, T. S. Rahman, B. Roldan Cuenya, *ACS Nano* 2014, *8*, 6671 – 6681.
8. E. Laborda, A. Molina, V. F. Espin, F. Martinez-Ortiz, J. Garcia de la Torre, R. G. Compton, *Angew. Chem. Int. Ed.* 2017, *56*, 782 – 785; *Angew. Chem.* 2017, *129*, 800 – 803.
9. X. Li, J. Iocozzia, Y. Chen, S. Zhao, X. Cui, W. Wang, H. Yu, S. Lin, Z. Lin, *Angew. Chem. Int. Ed.* 2018, *57*, 2046 – 2070; *Angew. Chem.* 2018, *130*, 2066 – 2093.
10. K. J. Stevenson, K. Tschulik, *Curr. Opin. Electrochem.* 2017, *6*, 38 – 45.
11. S. V. Sokolov, S. Eloul, E. Kätelhön, C. Batchelor-McAuley, R. G. Compton, *Phys. Chem. Chem. Phys.* 2017, *19*, 28– 43.
12. Z. Deng, R. Elattar, F. Maroun, C. Renault, *Anal. Chem.* 2018, *90*, 12923 – 12929.
13. B. M. Quinn, P. G. van't Hof, S. G. Lemay, *J. Am. Chem. Soc.* 2004, *126*, 8360 – 8361.
14. X. Xiao, A. J. Bard, *J. Am. Chem. Soc.* 2007, *129*, 9610 – 9612.
15. Y.-G. Zhou, N. V. Rees, R. G. Compton, *Angew. Chem. Int. Ed.* 2011, *50*, 4219 – 4221; *Angew. Chem.* 2011, *123*, 4305 – 4307.
16. H. Zhao, E. P. Douglas, B. S. Harrison, K. S. Schanze, *Langmuir* 2001, *17*, 8428 – 8433.

17. A. Guiet, T. Reier, N. Heidary, D. Felkel, B. Johnson, U. Vainio, H. Schlaad, Y. Aksu, M. Driess, P. Strasser, et al., *Chem. Mater.* 2013, *25*, 4645 – 4652.
18. M. Wuithschick, B. Paul, R. Bienert, A. Sarfraz, U. Vainio, M. Sztucki, R. Kraehnert, P. Strasser, K. Rademann, F. Emmerling, et al., *Chem. Mater.* 2013, *25*, 4679 – 4689.
19. J. Zhang, Y. Gao, R. A. Alvarez-Puebla, J. M. Buriak, H. Fenniri, *Adv. Mater.* 2006, *18*, 3233 – 3237.
20. Y. E. Jeun, B. Baek, M. W. Lee, H. S. Ahn, *Chem. Commun.* 2018, *54*, 10052 – 10055.
21. J. E. Dick, C. Renault, B.-K. Kim, A. J. Bard, *Angew. Chem. Int. Ed.* 2014, *53*, 11859 – 11862; *Angew. Chem.* 2014, *126*, 12053 – 12056.
22. M. W. Glasscott, A. D. Pendergast, J. E. Dick, *ACS Appl. Nano Mater.* 2018, *1*, 5702 – 5711.
23. J. Kim, J. E. Dick, A. J. Bard, *Acc. Chem. Res.* 2016, *49*, 2587 – 2595.
24. B.-K. Kim, A. Boika, J. Kim, J. E. Dick, A. J. Bard, *J. Am. Chem. Soc.* 2014, *136*, 4849 – 4852.
25. H. Deng, J. E. Dick, S. Kummer, U. Kragl, S. H. Strauss, A. J. Bard, *Anal. Chem.* 2016, *88*, 7754 – 7761.
26. H. Tsai, E. Hu, K. Perng, M. Chen, J.-C. Wu, Y.-S. Chang, *Surf. Sci.* 2003, *537*, L447 – L450.
27. Y.-G. Zhou, N. V. Rees, J. Pillay, R. Tshikhudo, S. Vilakazi, R. G. Compton, *Chem. Commun.* 2012, *48*, 224 – 226.
28. K. Tschulik, B. Haddou, D. Omanović, N. V. Rees, R. G. Compton, *Nano Res.* 2013, *6*, 836 – 841.
29. Y. Wang, E. Laborda, K. Tschulik, C. Damm, A. Molina, R. G. Compton, *Nanoscale* 2014, *6*, 11024 – 11030.